

FILE COPY  
NO. 5

TECHNICAL NOTES

NATIONAL ADVISORY COMMITTEE FOR AERONAUTICS

---

No. 730

---

WIND-TUNNEL INVESTIGATION OF EFFECT OF YAW ON  
LATERAL-STABILITY CHARACTERISTICS  
II - RECTANGULAR N.A.C.A. 23012 WING WITH A  
CIRCULAR FUSELAGE AND A FIN

By M. J. Damber and R. O. House  
Langley Memorial Aeronautical Laboratory

THIS DOCUMENT ON LOAN FROM THE FILES OF

NATIONAL ADVISORY COMMITTEE FOR AERONAUTICS  
LANGLEY AERONAUTICAL LABORATORY  
LANGLEY FIELD, HAMPTON, VIRGINIA

---

RETURN TO THE ABOVE ADDRESS.

REQUESTS FOR PUBLICATIONS SHOULD BE ADDRESSED  
AS FOLLOWS:

NATIONAL ADVISORY COMMITTEE FOR AERONAUTICS  
1724 F STREET, N.W.,  
WASHINGTON 25, D.C.

Washington  
September 1939



3 1176 01425 7217

NATIONAL ADVISORY COMMITTEE FOR AERONAUTICS

TECHNICAL NOTE NO. 730

WIND-TUNNEL INVESTIGATION OF EFFECT OF YAW ON  
LATERAL-STABILITY CHARACTERISTICS  
II - RECTANGULAR N.A.C.A. 23012 WING WITH A  
CIRCULAR FUSELAGE AND A FIN

By M. J. Bamber and R. O. House

SUMMARY

An N.A.C.A. 23012 rectangular wing with rounded tips was tested in combination with a fuselage of circular cross section at several angles of yaw in the N.A.C.A. 7-by 10-foot wind tunnel. The model was tested as a high-wing, a midwing, and a low-wing monoplane; for each wing location, tests were made with two amounts of dihedral and with partial-span split flaps. For each combination of wing and fuselage, tests were made with and without a fin. Sample charts of the coefficients of rolling moment  $C_l'$ , yawing moment  $C_n'$ , and lateral force  $C_y'$  are given for some of the combinations tested. The rate of change in the coefficients with angle of yaw  $\psi'$  is given for stability calculation.

The value of the effect on  $dC_l'/d\psi'$  of wing-fuselage interference change sign as the wing was moved downward on the fuselage from the high to the low position, being zero at some intermediate position. In general, the change in  $dC_l'/d\psi'$  for a given change in the dihedral was only slightly affected by wing-fuselage interference. Moving the wing from the low to the high position generally tended to increase the value of  $dC_l'/d\psi'$  and  $dC_n'/d\psi'$  and to decrease the effectiveness of the fin on  $dC_l'/d\psi'$ ,  $dC_n'/d\psi'$ , and  $dC_y'/d\psi'$ .

INTRODUCTION

Estimation of the stability characteristics of airplanes can be made only if the stability derivatives of

the particular airplane are known. Mathematical equations are available and convenient charts are given in reference 1 for predicting the lateral-stability characteristics of airplanes. Some of the factors affecting the values of these derivatives are wing, fuselage, and fin forms and the aerodynamic interference between these parts.

The effects on the lateral-stability characteristics that depend on yaw of several wing forms, changes in tip shape, dihedral, taper, wing section, sweep angle, and split flaps are given in references 2 and 3. A theoretical prediction of some of the lateral-stability characteristics for wings is given in reference 4. The purpose of the present investigation was to obtain information relative to the interference effects on lateral-stability characteristics of wing-fuselage-fin combinations. Tests were made with a fuselage of circular cross section having a removable fin; the fuselage was tested separately and in combination with the N.A.C.A. 23012 rectangular wing, for which results of a similar investigation are given in reference 3. The wing variables were dihedral and flap deflection for each of three locations representing a low-wing, a midwing, and a high-wing monoplane. The effect of the fin was obtained for each variation of each fuselage-wing combination.

This paper gives the lateral-stability characteristics of the wing-fuselage-fin combinations tested and the variations with yaw in rolling-moment, yawing-moment, and side-force coefficients for the combinations.

#### APPARATUS AND MODELS

The tests were made in the N.A.C.A. 7- by 10-foot wind tunnel with the regular-6-component balance. The closed-throat tunnel is described in reference 5 and the balance is described in reference 6.

Figure 1 is a drawing of the laminated mahogany model. The rectangular wing was used for the tests reported in reference 3. The tip plan form of the wing is composed of two quadrants of similar ellipses. The N.A.C.A. 23012 profile is maintained to the end of the wing and, in elevation, the maximum upper-surface section ordinates are in one plane. The wing was set at  $0^\circ$  incidence in all positions. The fuselage is circular in

cross section and was made from the dimensions given in reference 7 for the circular fuselage.

The fin was made to the N.A.C.A. 0009 section and, in plan form, is representative of the fins used on the average airplane. The area of the fin is 45 square inches; the ratio of fin area to wing area is 0.08; the aspect ratio of the fin is 2; and the distance from the assumed position of the center of gravity of the model to the trailing edge of the fin is 0.455 times the wing span.

The 20-percent-chord split flap, made of 1/16-inch steel plate, is attached to the wing at an angle of 60° and extends over 60 percent of the span at the center section. For the midwing and the high-wing positions, the center section of the flap was cut away to allow for the fuselage. The gap between the flap and the fuselage was sealed for all conditions.

#### TESTS

The fuselage was tested alone and in combination with the wing as a high-wing, a midwing, and a low-wing monoplane. For each wing position, the combination was tested with 0° and 5° dihedral and with the split flap deflected 0° and 60°. For all fuselage-wing combinations, tests were made both with and without the fin.

Every model combination was tested at angles of yaw of 0°, ±1°, ±2°, ±3°, ±5°, 7°, ±10°, and 15°. At each angle of yaw, tests were made at angles of attack of -5°, 5°, and 15° for a flap deflection of 0° and at angles of attack of -10°, 0°, and 10° for a flap deflection 60°. Tests were also made for all model combinations at 2° intervals of angle of attack from -10° to the stall at yaw angles of -5° and 5°.

The tests were made at a dynamic pressure of 16.37 pounds per square foot, which corresponds to an air speed of about 80 miles per hour under standard conditions. The test Reynolds Number was about 609,000 based on the chord of the wing.

## RESULTS

The data, with primes to indicate wind axes, are given in standard nondimensional coefficient form. The coefficients for the fuselage are based on the wing dimensions.

$C_Y'$ , lateral-force coefficient ( $Y'/qS$ ).

$C_l'$ , rolling-moment coefficient ( $L'/qSb$ ).

$C_n'$ , yawing-moment coefficient ( $N'/qSb$ ).

where  $Y'$  is lateral force.

$L'$ , rolling moment.

$N'$ , yawing moment.

$q$ , dynamic pressure ( $1/2 \rho V^2$ ).

$V$ , tunnel-air velocity.

$\rho$ , air density.

$S$ , wing area.

$b$ , wing span.

and  $\alpha$  is angle of attack.

$c$ , chord.

$\psi'$ , angle of yaw, degrees (positive when the model is yawed to the right).

$\Gamma$ , dihedral angle of plane of section chord lines exclusive of tip portion.

$\delta_f$ , flap deflection.

The forces and the moments have been given with respect to the wind-tunnel system of axes that intersect in the model at the center-of-gravity location shown in figure 1.

The lateral force, the rolling moment, and the yawing moment were corrected for initial asymmetry by deduct-

ing the values obtained without yaw from the values obtained with yaw. The coefficients were plotted against angle of yaw; figures 2 to 7 are sample plots.

The stability characteristics,  $\left(\frac{dC_{l'}}{d\psi'}\right)_{c.g.}$ ,

$\left(\frac{dC_{n'}}{d\psi'}\right)_{c.g.}$ , and  $\left(\frac{dC_{y'}}{d\psi'}\right)_{c.g.}$ , were obtained by meas-

uring at zero yaw the slope of the curves of the coefficients against angle of yaw. These values are given as tailed points in figures 8 to 20. The values given as untailed points were obtained from data measured at  $\psi' = \pm 5^\circ$  ( $\alpha$  variable) by assuming that the coefficients had a straight-line variation for the range from  $5^\circ$  to  $-5^\circ$  yaw. The values obtained by this method are within the practical limits of accuracy for the range of low angles of attack. For some cases at the higher angles of attack, the values are considerably different when there are large departures from the straight-line variation of the coefficients with yaw and when breaks occur in the curves as shown in figures 2 to 7. The breaks in the curves sometimes indicate that the wing is partly stalled for some angles of yaw. For angles of attack near the stall, the variation of the stability characteristics with angle of attack is expected to be discontinuous depending upon the critical manner in which the wing stalls. The variation of the stability characteristics with wing location is shown for a condition of medium angles of attack in figures 21 and 22. The values for the wing alone given in figures 8 to 22 were obtained from reference 3 and were converted to the center of gravity of the complete model.

## DISCUSSION

The tests for which angle of attack was used as a variable were made primarily to insure that the variation of the stability characteristics with angle of attack was not irregular in the  $10^\circ$  angle-of-attack interval used in the tests for which yaw was a variable. The curves in figures 8 to 20 show that the stability characteristics change gradually with angle of attack except for the angles of attack near the stall, where the values are known to be irregular or indeterminate.

The curves in figures 21 and 22 are given to show the general variation of the stability characteristics with wing position. Although corresponding curves for other conditions will be somewhat similar, the actual values change considerably with angle of attack. It should be remembered that the data are for a fixed vertical tail; no rudder deflections were possible.

Wing and fuselage.- The value of the change of  $dC_l'/d\psi'$  with  $\Gamma$  varied considerably for different wing-fuselage combinations, although the average was about the same as that obtained for wings alone, 0.00021 per degree (reference 3). In general, increasing  $\Gamma$  algebraically increased  $dC_m'/d\psi'$ ; the amount, however, was small. No regular change in  $dC_y'/d\psi'$  with  $\Gamma$  was shown.

The values of  $dC_l'/d\psi'$  usually decreased algebraically as the wing was moved from the high to the low position, as is shown in figures 21 and 22. With the wing in the midposition, the effect on  $dC_l'/d\psi'$  of wing-fuselage interference was small, being equivalent to an increase in dihedral of less than  $1^\circ$  for most of the angle-of-attack range. With the wing in the high position, the interference was equivalent to an increase in effective dihedral of about  $3^\circ$  to  $5^\circ$ . In the low position, the interference effect changed considerably with angle of attack.

The effect on  $dC_n'/d\psi'$  of wing-fuselage interference was small and acted to reduce the instability of the fuselage. The interference generally increased as the wing was moved from the high to the low position.

The values of  $dC_y'/d\psi'$  were quite appreciably affected by flap deflection. With the wing in the midposition with zero dihedral and flaps undeflected, the wing-fuselage interference was negligible but increased when the wing was moved to either the high or the low position and also when the dihedral was increased. With the flaps deflected, the interference effects were negative, tending to reduce the lateral force. The magnitude of the interference was greatest when the wing was in the midposition, the resultant lateral force being approximately zero. This characteristic cannot be explained, but it may have some effect on the sideslipping characteristics with different flap deflections.

Fin and fuselage.- The characteristics of the fuselage-fin combination are shown in figure 8. The value of the increase in  $dC_Y'/d\psi'$  is slightly larger than would be expected of an airfoil of the same aspect ratio as the fin but without the fuselage interference (reference 8). The change in  $dC_l'/d\psi'$  with angle of attack is of the order expected from  $dC_Y'/d\psi'$  and the vertical-tail position; the change in  $dC_n'/d\psi'$  produced by the fin is somewhat less than would be expected from the change in  $dC_Y'/d\psi'$  and the tail length.

Wing, fuselage, and fin.- The contribution of the fin to  $dC_l'/d\psi'$  is equivalent to an increase in dihedral of from  $1^\circ$  to  $4^\circ$  (figs. 8, 21, and 22). Although of interest in relation to inherent stability, this contribution should not be counted when dihedral for maneuvering is considered because a movement of the rudder to obtain sideslip will act to counteract this effective dihedral.

The effectiveness of the fin in changing  $dC_n'/d\psi'$  and  $dC_Y'/d\psi'$  was dependent upon wing position, angle of attack, and flap angle. Moving the wing downward on the fuselage increased the effectiveness of the fin, the maximum effectiveness being greater than that of the fin and the fuselage without the wing. No explanation of this result is forthcoming at present. A number of possibilities were considered, such as angle of attack, wing wake, influence of the wing-tip vortices, and turbulence effects. These effects, however, should vary with angle of attack and no such large variation was shown by the results.

## CONCLUSIONS

1. The value of the wing-fuselage interference effect on  $dC_l'/d\psi'$ , the slope of the curve of rolling-moment coefficient against yaw, was small when the wing was mounted in the midposition, being equivalent to an increase in effective dihedral of about  $1^\circ$  or less.

2. When the wing was shifted to the high position, the wing-fuselage interference on  $dC_l'/d\psi'$  increased, being equivalent to an increase in dihedral of the order of  $4^\circ$ ; with the wing in the low position, the interference varied considerably with angle of attack.



3. The change in  $dC_l'/d\psi'$  for a given change in wing dihedral was generally not greatly affected by the wing-fuselage interference.

4. With flaps deflected, the wing-fuselage interference appreciably reduced the lateral force; without flaps, this interference was negligible.

5. The effectiveness of the fin on  $dC_n'/d\psi'$ , the slope of the curve of yawing-moment coefficient against yaw, increased as the wing was moved downward on the fuselage, the maximum effectiveness being greater than that of the fuselage-fin combination and occurring with flaps deflected.

6. Moving the wing downward on the fuselage generally tended to increase the effectiveness of the fin on  $dC_l'/d\psi'$  and on  $dC_y'/d\psi'$ , the slope of the curve of lateral-force coefficient against yaw.

Langley Memorial Aeronautical Laboratory,  
National Advisory Committee for Aeronautics,  
Langley Field, Va., August 22, 1939.

## REFERENCES

1. Zimmerman, Charles H.: An Analysis of Lateral Stability in Power-Off Flight with Charts for Use in Design. T.R. No. 589, N.A.C.A., 1937.
2. Shortal, Joseph A.: Effect of Tip Shape and Dihedral on Lateral-Stability Characteristics. T.R. No. 548, N.A.C.A., 1935.
3. Damber, M. J., and House, R. O.: Wind-Tunnel Investigation of Effect of Yaw on Lateral-Stability Characteristics. I - Four N.A.C.A. 23012 Wings of Various Plan Forms with and without Dihedral. T.N. No. 703, N.A.C.A., 1939.
4. Pearson, Henry A., and Jones, Robert T.: Theoretical Stability and Control Characteristics of Wings with Various Amounts of Taper and Twist. T.R. No. 635, N.A.C.A., 1938.
5. Wenzinger, Carl J., and Harris, Thomas A.: Wind-Tunnel Investigation of an N.A.C.A. 23012 Airfoil with Various Arrangements of Slotted Flaps. T.R. No. 664, N.A.C.A., 1939.
6. Harris, Thomas A.: The 7 by 10 Foot Wind Tunnel of the National Advisory Committee for Aeronautics. T.R. No. 412, N.A.C.A., 1931.
7. Jacobs, Eastman N., and Ward, Kenneth E.: Interference of Wing and Fuselage from Tests of 209 Combinations in the N.A.C.A. Variable-Density Tunnel. T.R. No. 540, N.A.C.A., 1935.
8. Zimmerman, C. H.: Characteristics of Clark Y Airfoils of Small Aspect Ratios. T.R. No. 431, N.A.C.A., 1932.

A and B are quadrants of similar ellipses.

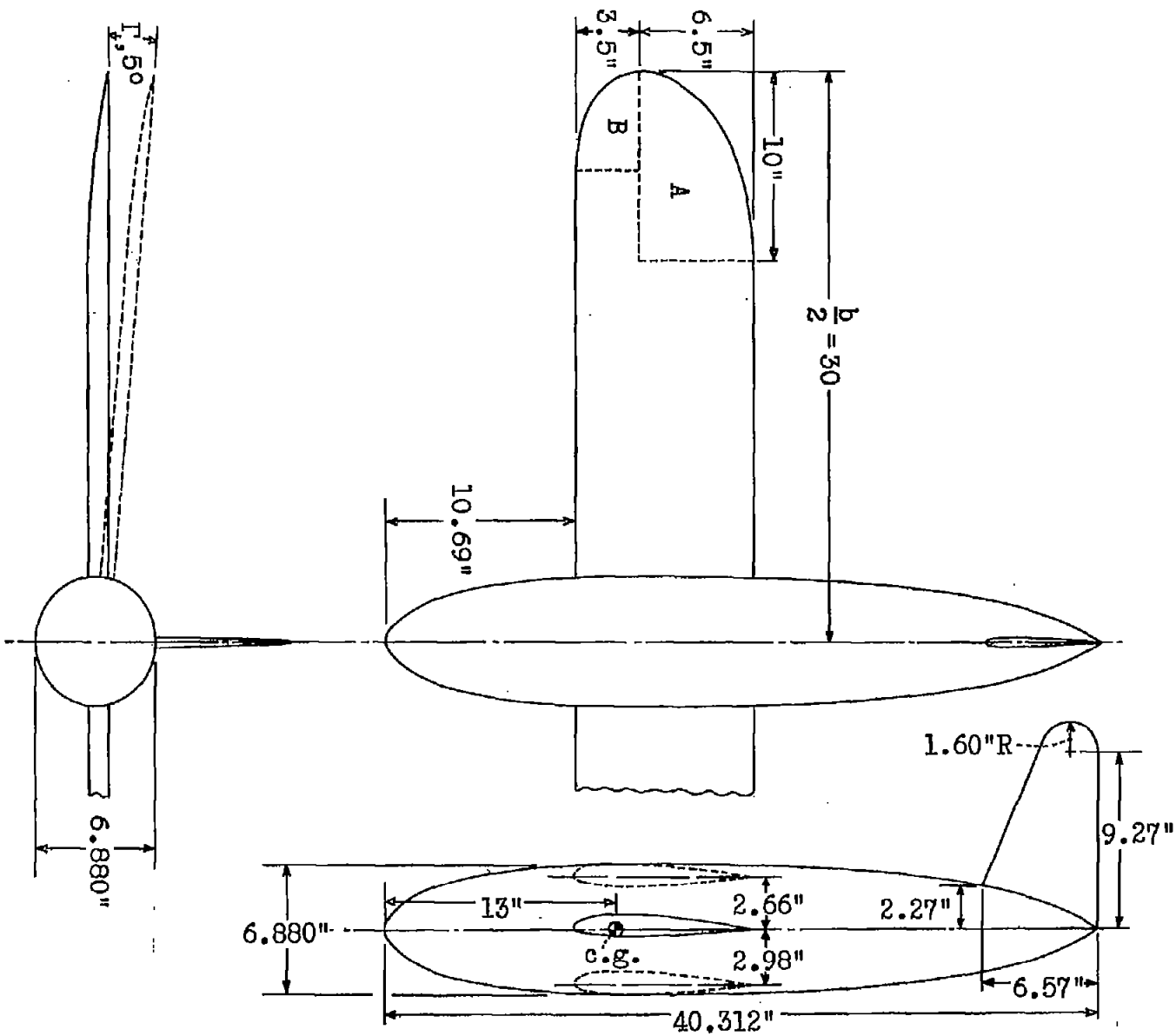


Figure 1.- Drawing of N.A.C.A. 23012 wing in combination with circular fuselage and fin of N.A.C.A. 0009 section.

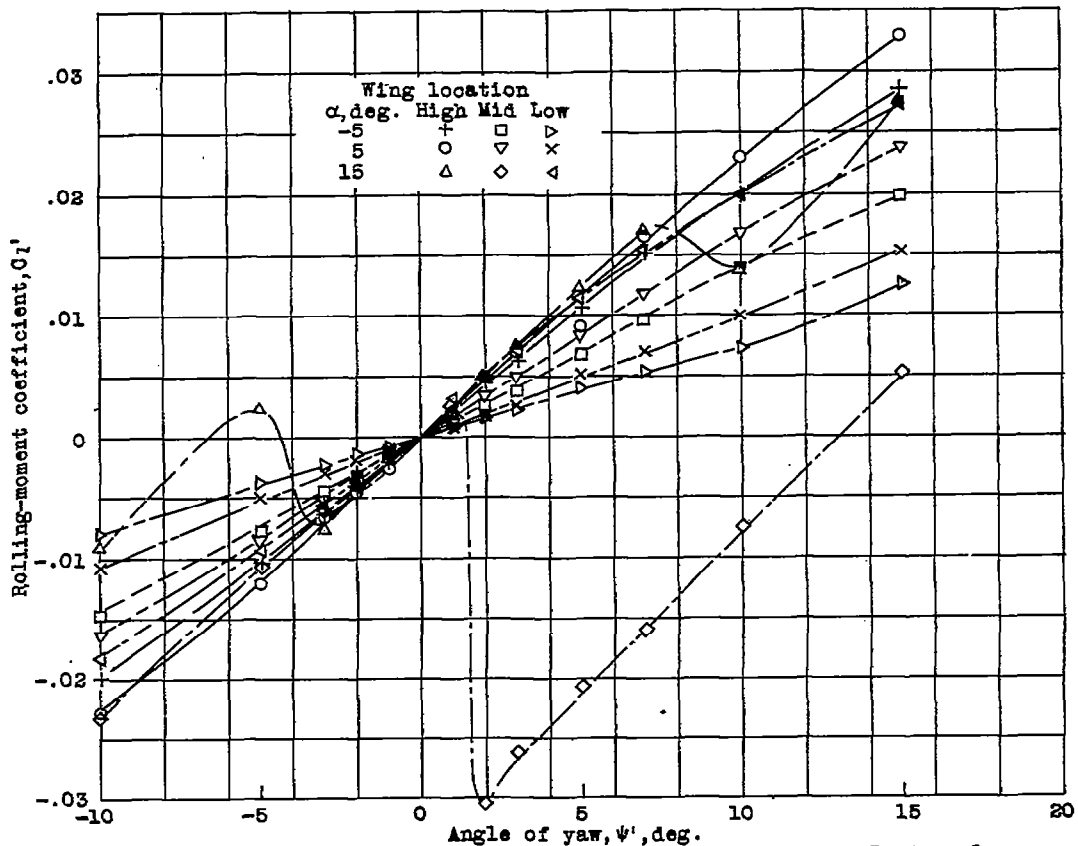


Figure 2.- Variation of rolling-moment coefficient with yaw. Rectangular N.A.C.A. 23012 wing with rounded tips in combination with circular fuselage;  $\Gamma, 5^\circ; \delta_r, 0^\circ$ .

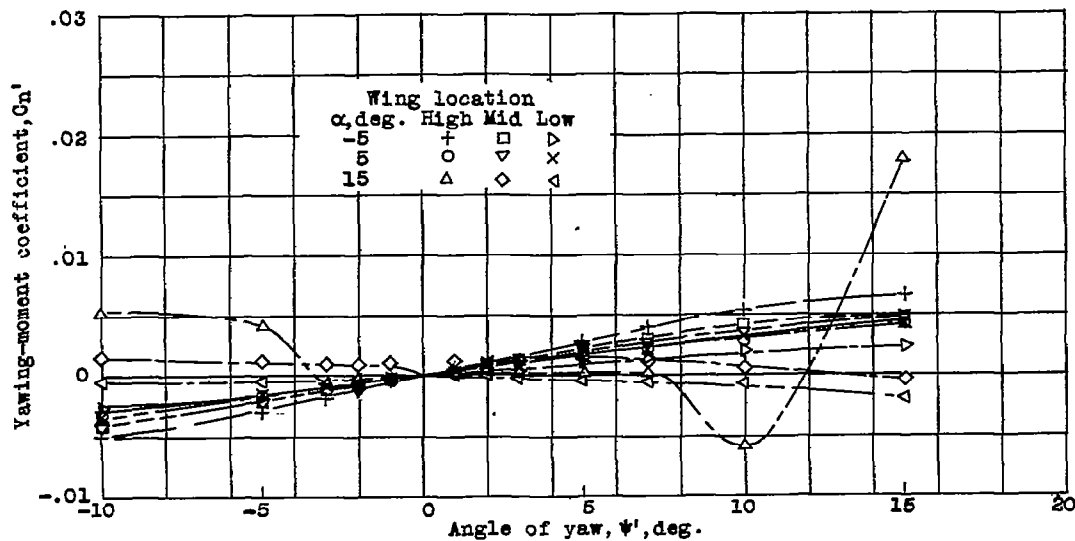


Figure 3.- Variation of yawing-moment coefficient with yaw. Rectangular N.A.C.A. 23012 wing with rounded tips in combination with circular fuselage;  $\Gamma, 5^\circ; \delta_r, 0^\circ$ .

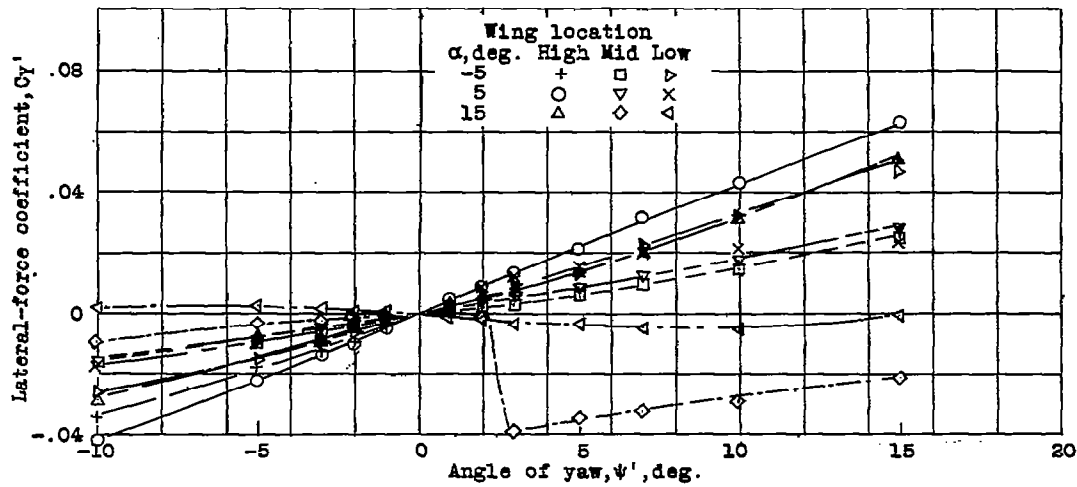


Figure 4.- Variation of lateral-force coefficient with yaw. Rectangular N.A.C.A. 23012 wing with rounded tips in combination with circular fuselage;  $\Gamma, 5^\circ$ ;  $\delta_f, 0^\circ$ .

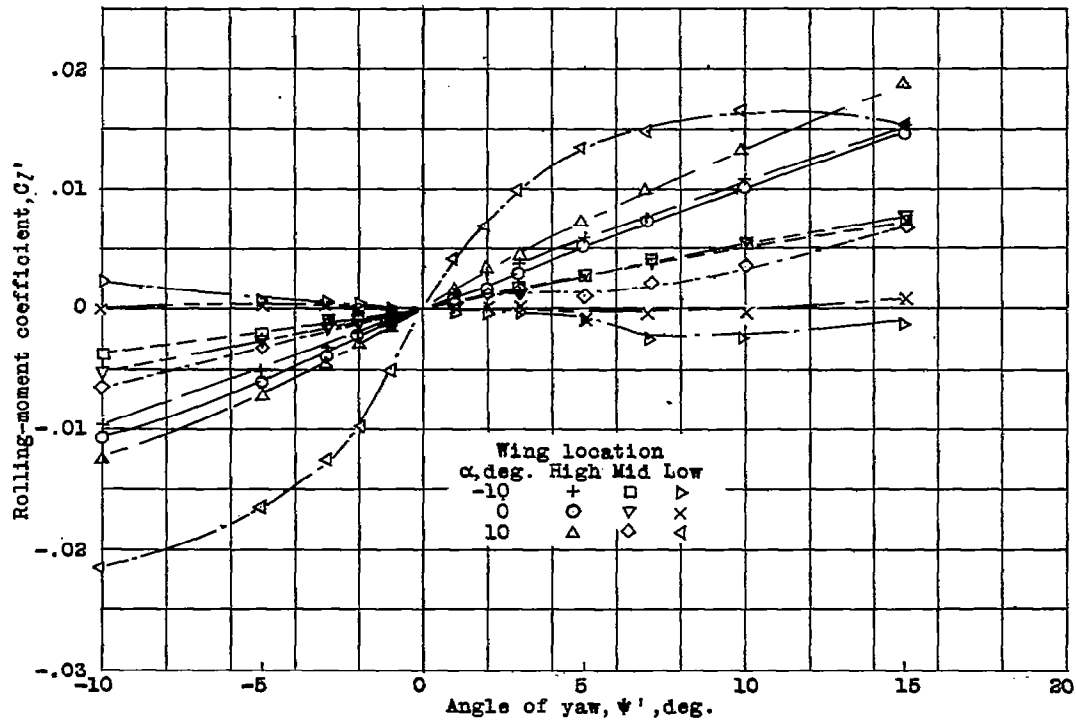


Figure 5.- Variation of rolling-moment coefficient with yaw. Rectangular N.A.C.A. 23012 wing with rounded tips in combination with circular fuselage;  $\Gamma, 0^\circ$ ;  $\delta_r, 80^\circ$ .

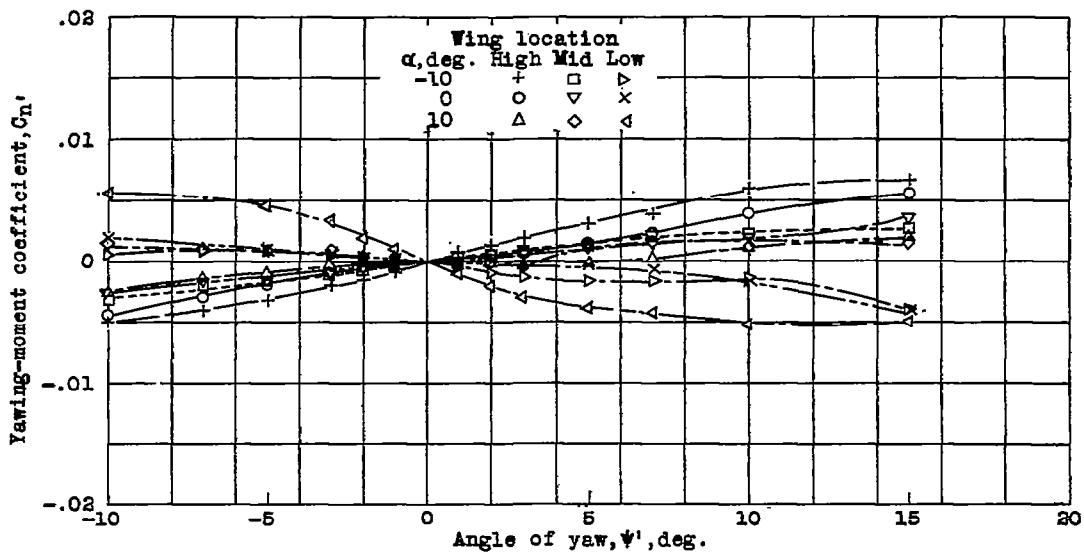


Figure 6.-Variation of yawing-moment coefficient with yaw. Rectangular N.A.C.A. 23012 wing with rounded tips in combination with circular fuselage;  $\Gamma, 0^\circ$ ;  $\delta_r, 60^\circ$ .

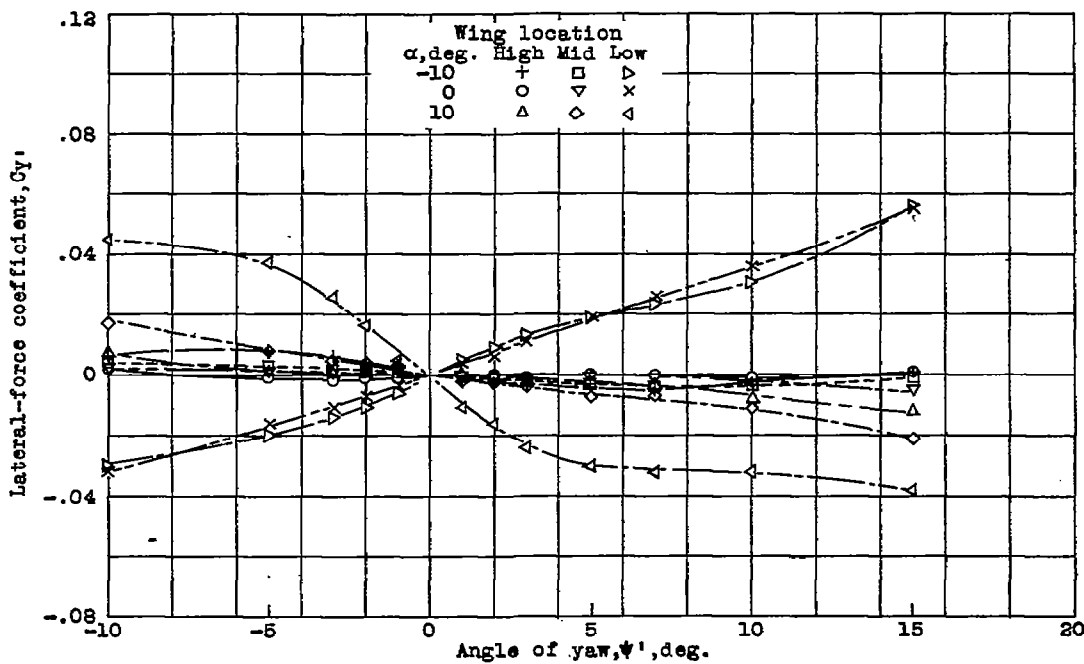


Figure 7.- Variation of lateral-force coefficient with yaw. Rectangular N.A.C.A. 23012 wing with rounded tips in combination with circular fuselage;  $\Gamma, 0^\circ$ ;  $\delta_r, 60^\circ$ .

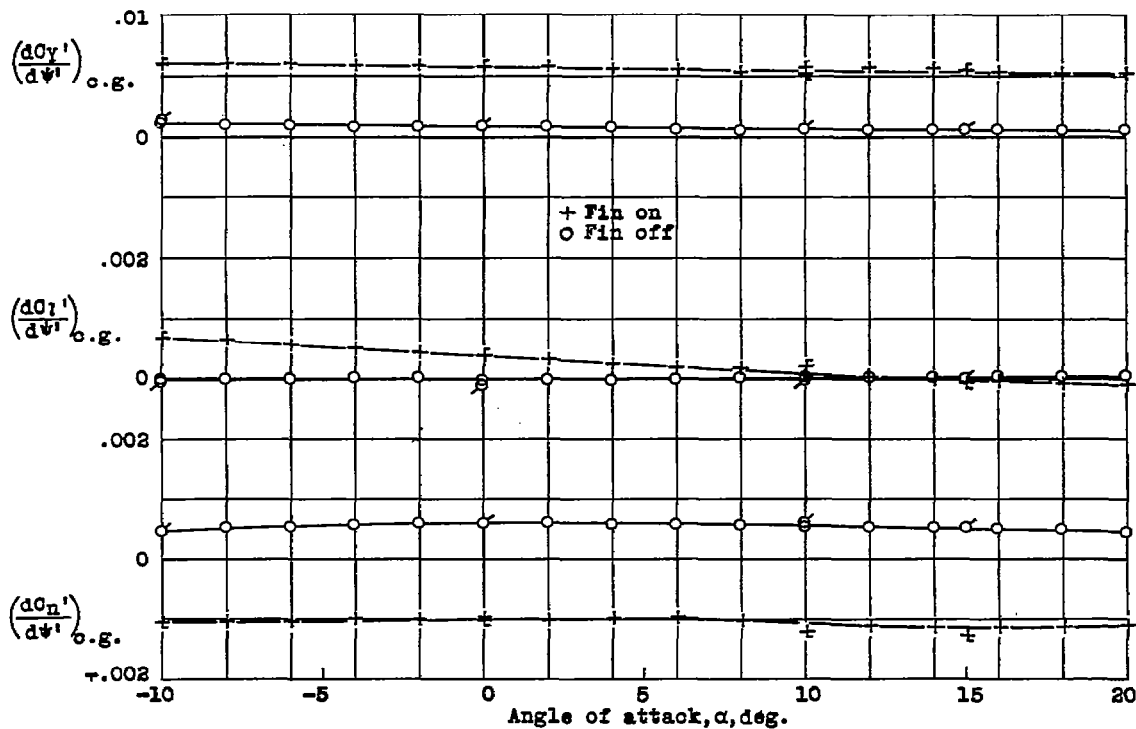


Figure 8.- Variation of  $\left(\frac{dC_{y1}}{d\psi_1}\right)_{c.g.}$ ,  $\left(\frac{dC_{z1}}{d\psi_1}\right)_{c.g.}$ , and  $\left(\frac{dC_{n1}}{d\psi_1}\right)_{c.g.}$  with angle of attack. Circular fuselage with and without fin.

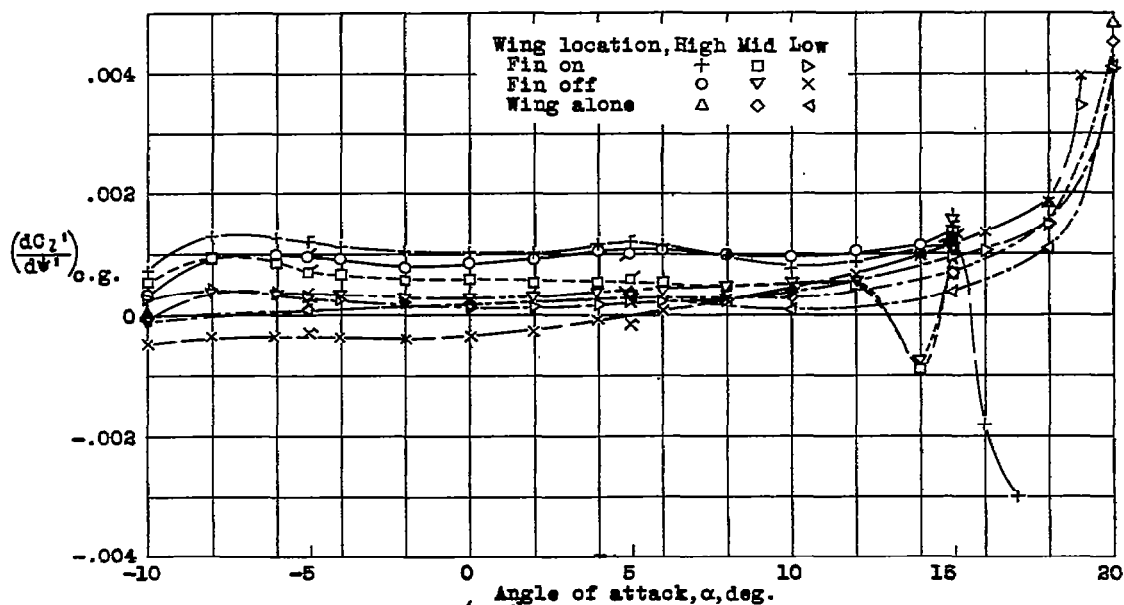


Figure 9.- Variation of  $\left(\frac{dC_{z1}}{d\psi_1}\right)_{c.g.}$  with angle of attack. Rectangular N.A.C.A. 23013 wing alone and in combination with circular fuselage with and without fin;  $\delta_2, 0^\circ$ ;  $\Gamma, 0^\circ$ .

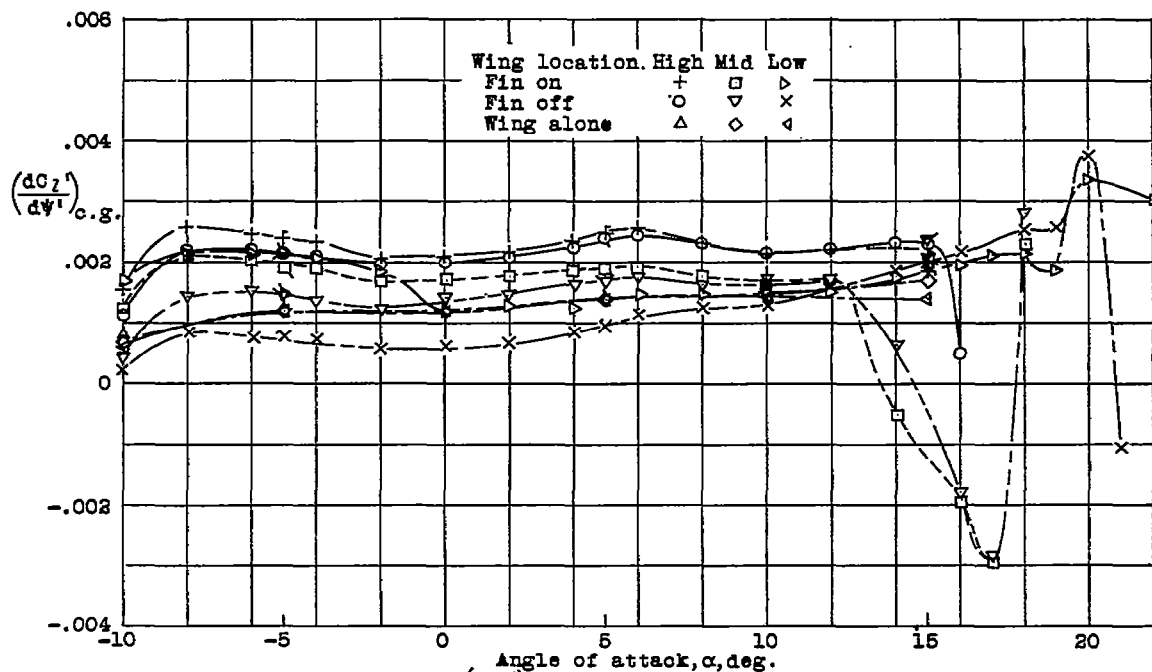


Figure 10.- Variation of  $(\frac{dC_L'}{d\psi'})_{c.g.}$  with angle of attack. Rectangular N.A.C.A. 23012 wing alone and in combination with circular fuselage with and without fin;  $\delta_f, 0^\circ$ ;  $\Gamma, 5^\circ$ .

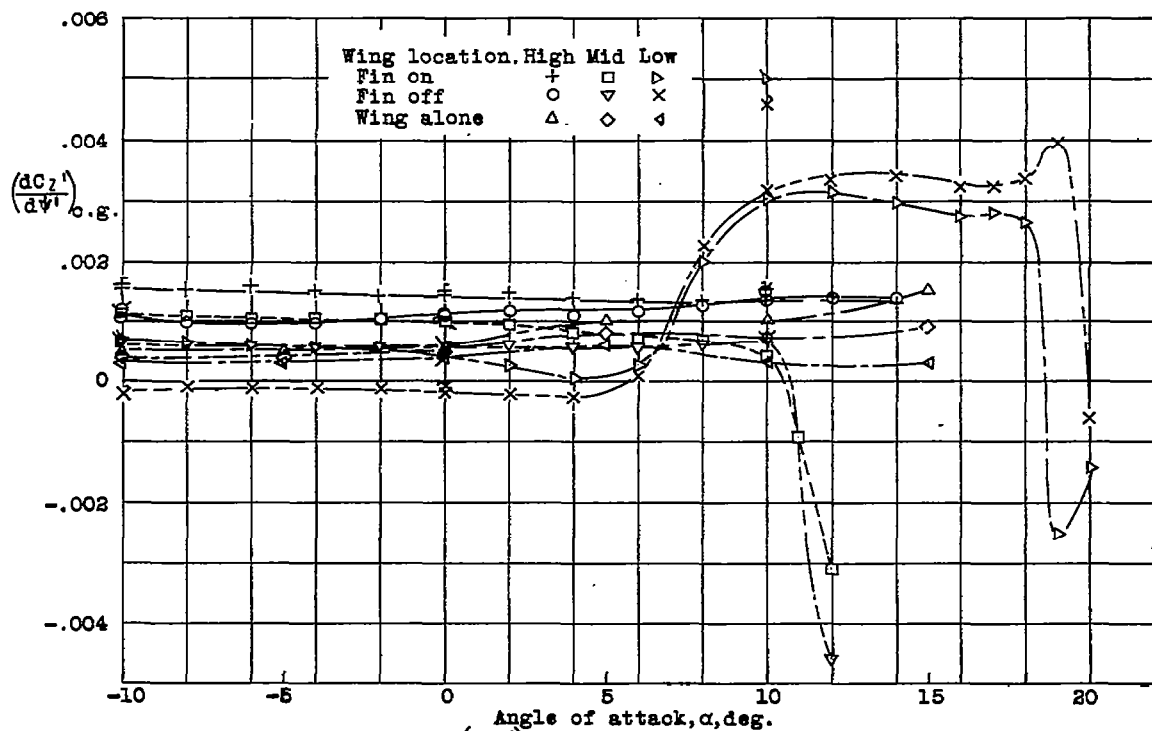


Figure 11.- Variation of  $(\frac{dC_L'}{d\psi'})_{c.g.}$  with angle of attack. Rectangular N.A.C.A. 23012 wing alone and in combination with circular fuselage with and without fin;  $\delta_f, 80^\circ$ ;  $\Gamma, 0^\circ$ .



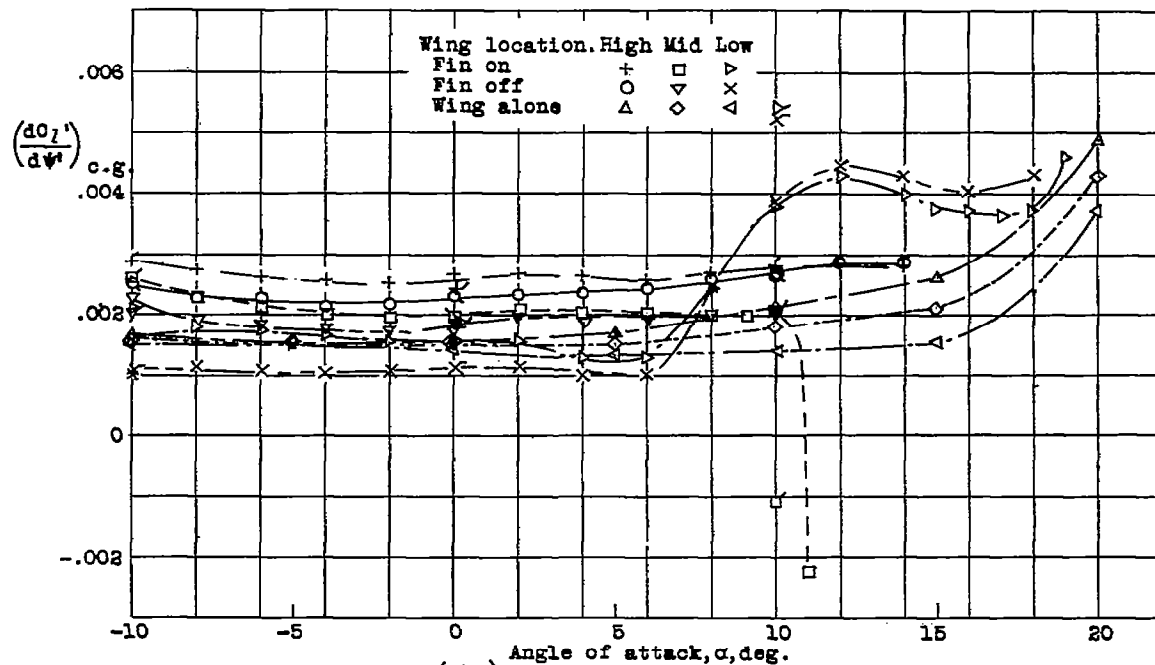


Figure 12.- Variation of  $\left(\frac{dC_{M1}'}{d\psi'}\right)_{c.g.}$  with angle of attack. Rectangular N.A.C.A. 23012 wing alone and in combination with circular fuselage with and without fin;  $\delta_f, 60^\circ$ ;  $\Gamma, 5^\circ$ .

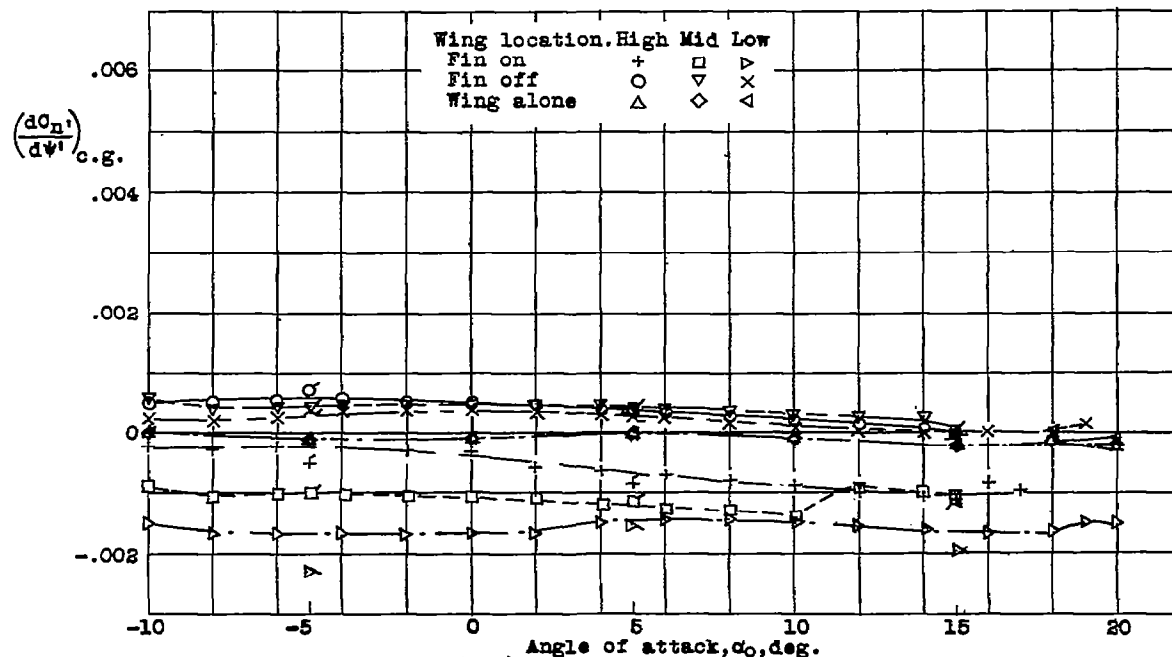


Figure 13.- Variation of  $\left(\frac{dC_{M1}'}{d\psi'}\right)_{c.g.}$  with angle of attack. Rectangular N.A.C.A. 23012 wing alone and in combination with circular fuselage with and without fin;  $\delta_f, 0^\circ$ ;  $\Gamma, 0^\circ$ .

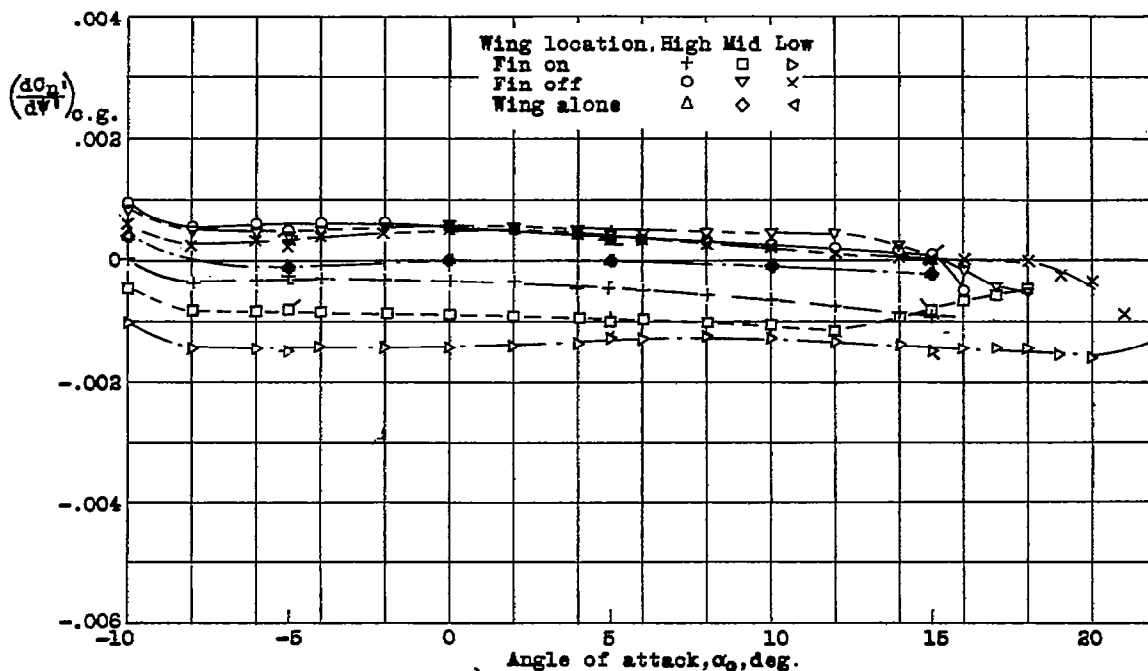


Figure 14.- Variation of  $(\frac{dC_{n1}}{d\alpha})_{c.g.}$  with angle of attack. Rectangular N.A.C.A. 23012 wing alone and in combination with circular fuselage with and without fin;  $\delta_f, 0^\circ$ ;  $\Gamma, 5^\circ$ .

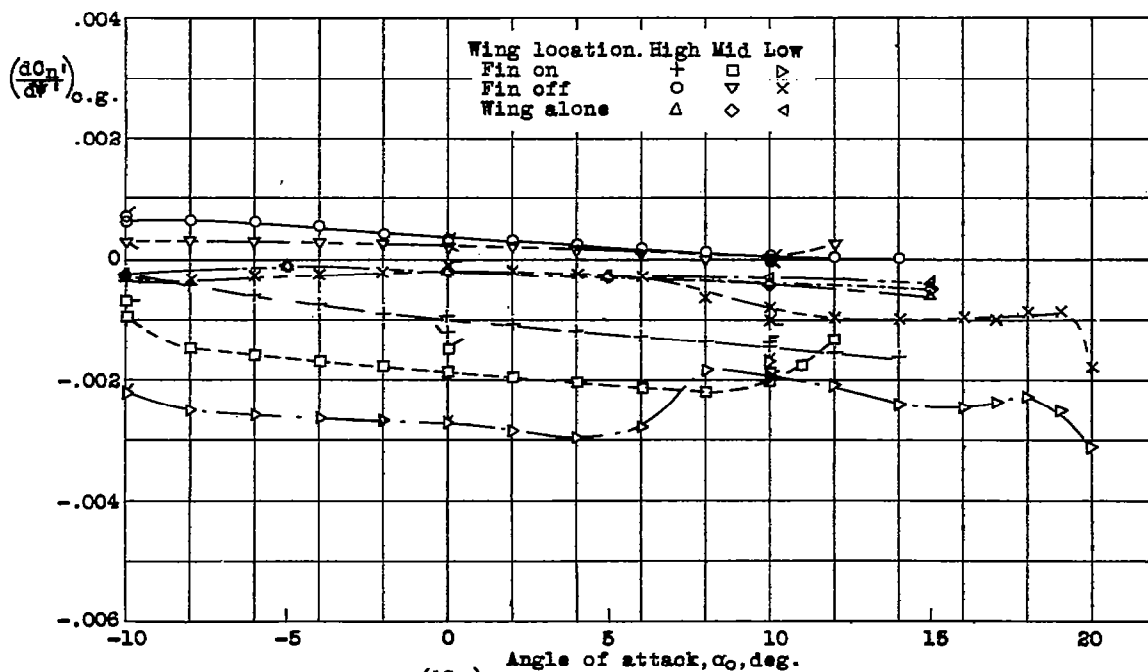


Figure 15.- Variation of  $(\frac{dC_{n1}}{d\alpha})_{c.g.}$  with angle of attack. Rectangular N.A.C.A. 23012 wing alone and in combination with circular fuselage with and without fin;  $\delta_f, 60^\circ$ ;  $\Gamma, 0^\circ$ .

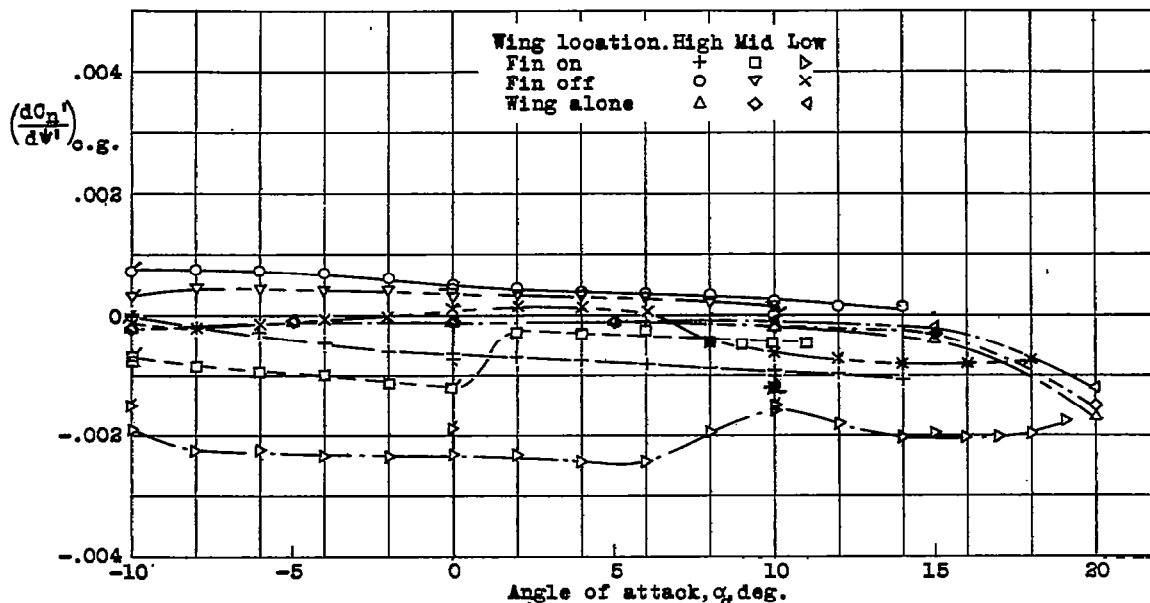


Figure 16.- Variation of  $(\frac{dC_n^\eta}{d\alpha^\eta})_{c.g.}$  with angle of attack. Rectangular N.A.C.A. 23012 wing alone and in combination with circular fuselage with and without fin;  $\delta_f, 60^\circ$ ;  $\Gamma, 5^\circ$ .

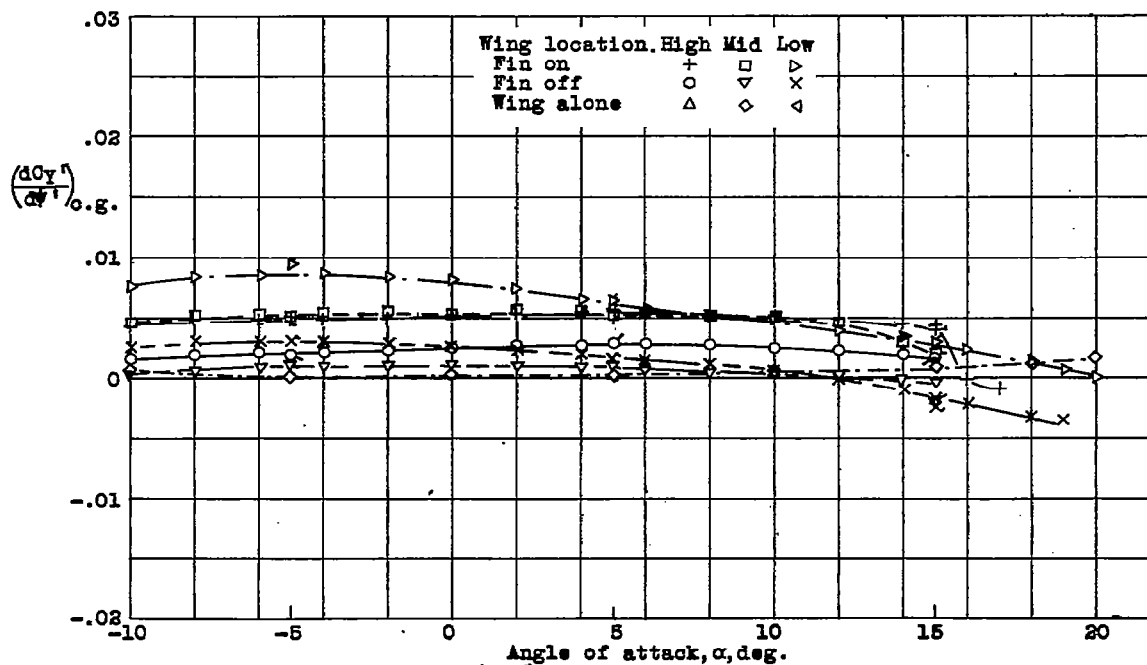


Figure 17.- Variation of  $(\frac{dC_y^\eta}{d\alpha^\eta})_{c.g.}$  with angle of attack. Rectangular N.A.C.A. 23012 wing alone and in combination with circular fuselage with and without fin;  $\delta_f, 0^\circ$ ;  $\Gamma, 0^\circ$ .

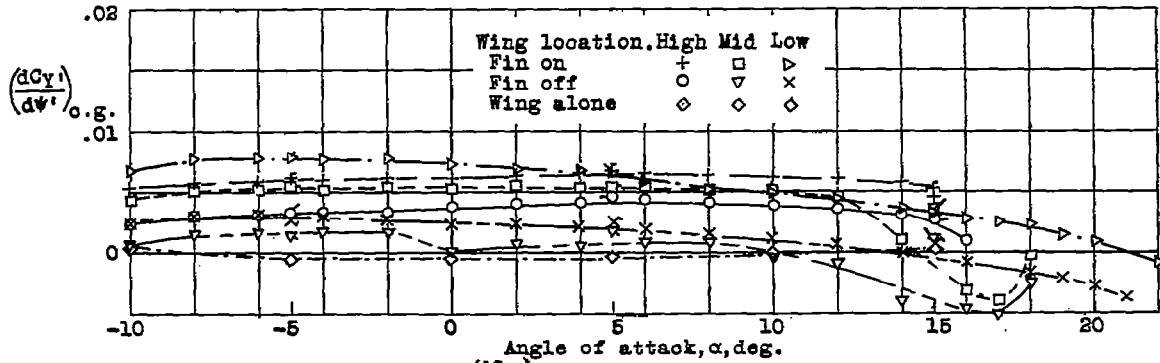


Figure 18.- Variation of  $(\frac{dC_{yl}}{d\psi'})_{c.g.}$  with angle of attack. Rectangular N.A.C.A. 23012 wing alone and in combination with circular fuselage with and without fin;  $\delta_f, 0^\circ$ ;  $\Gamma, 5^\circ$ .

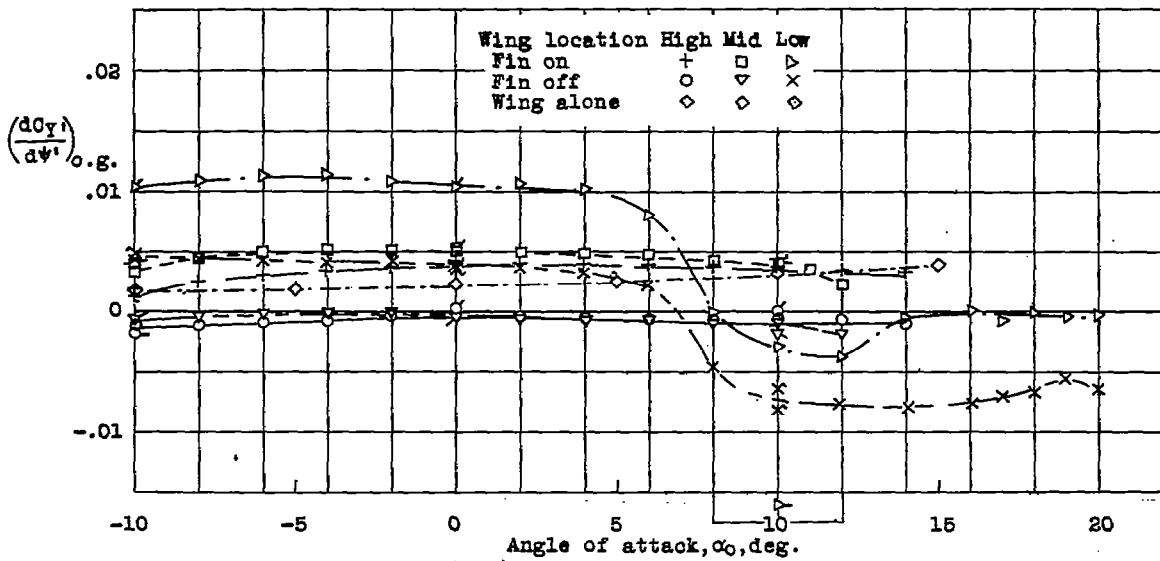


Figure 19.- Variation of  $(\frac{dC_{yl}}{d\psi'})_{c.g.}$  with angle of attack. Rectangular N.A.C.A. 23012 wing alone and in combination with circular fuselage with and without fin;  $\delta_f, 60^\circ$ ;  $\Gamma, 0^\circ$ .

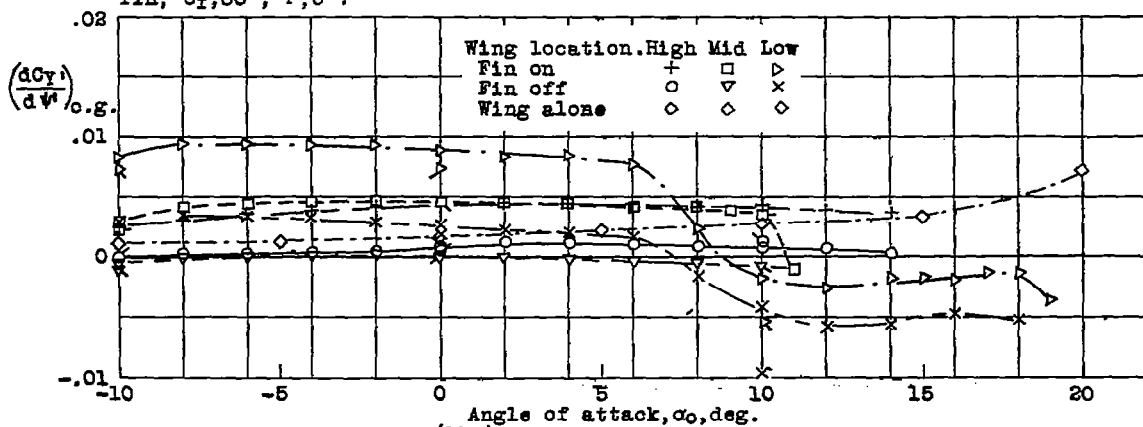


Figure 20.- Variation of  $(\frac{dC_{yl}}{d\psi'})_{c.g.}$  with angle of attack. Rectangular N.A.C.A. 23012 wing alone and in combination with circular fuselage with and without fin;  $\delta_f, 60^\circ$ ;  $\Gamma, 5^\circ$ .

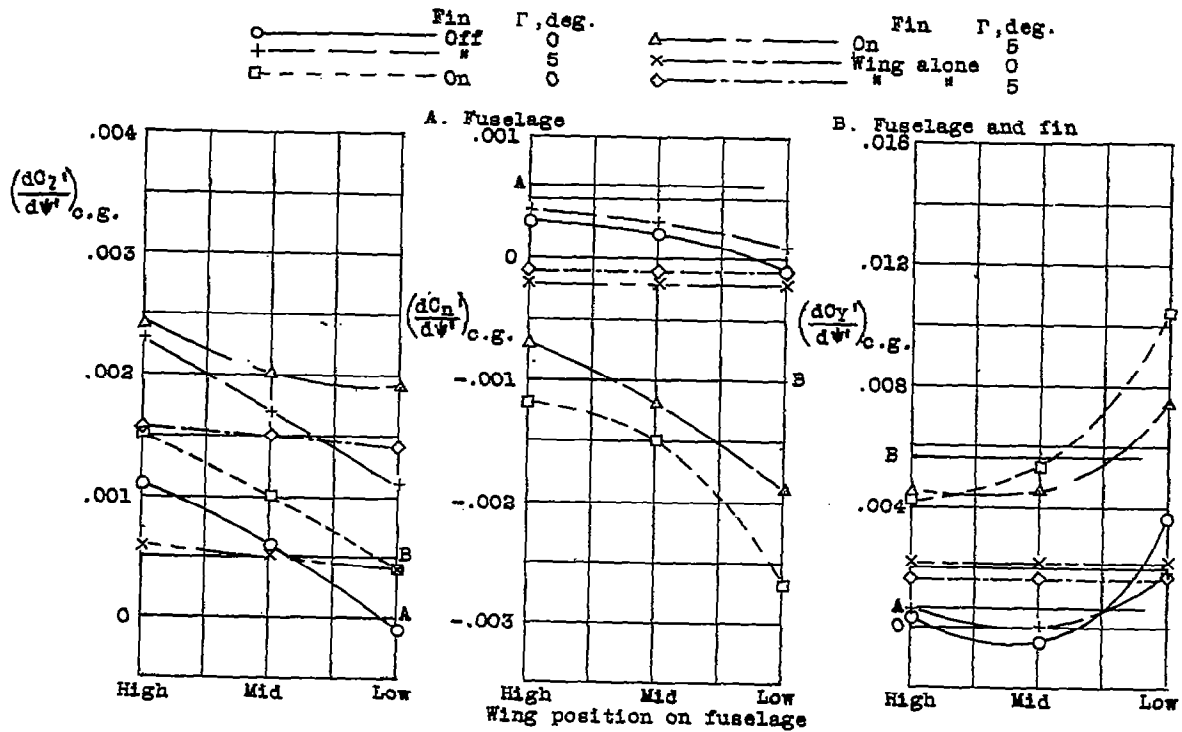


Figure 22.- Variation of  $(\frac{dC_{Z'}}{d\psi'})_{c.g.}$ ,  $(\frac{dC_{N'}}{d\psi'})_{c.g.}$ , and  $(\frac{dC_{Y'}}{d\psi'})_{c.g.}$  with wing position. Rectangular N.A.C.A. 23012 wing alone and in combination with circular fuselage with and without fin;  $\beta_r, 60^\circ$ ;  $\alpha, 0^\circ$ .

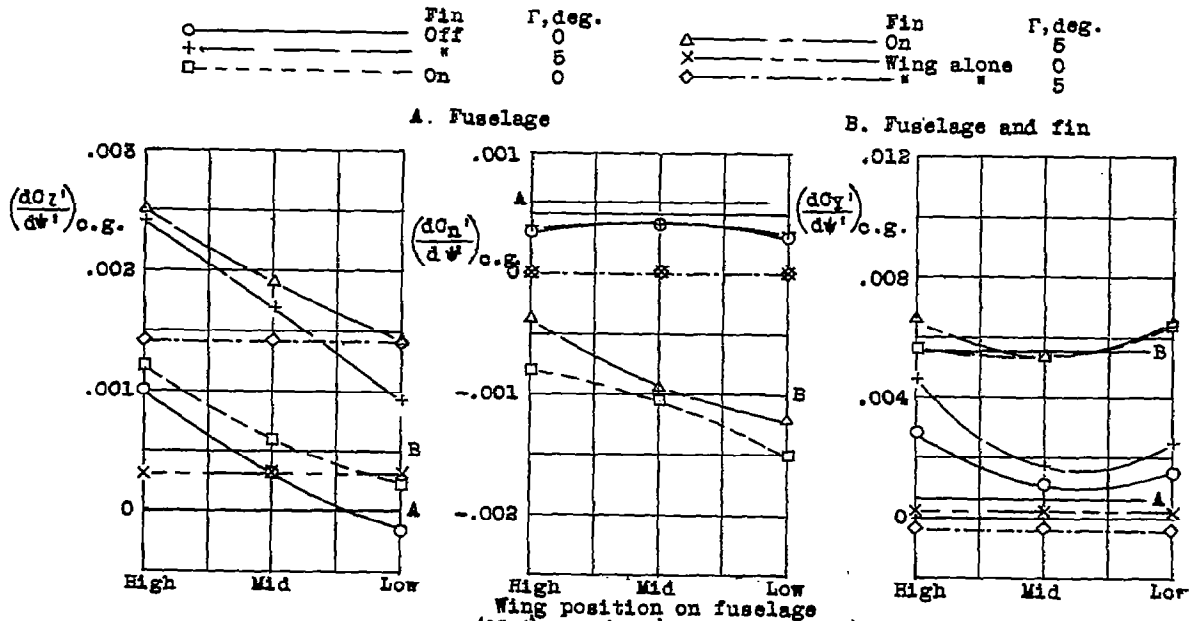


Figure 21.- Variation of  $(\frac{dC_{Z'}}{d\psi'})_{c.g.}$ ,  $(\frac{dC_{N'}}{d\psi'})_{c.g.}$ , and  $(\frac{dC_{Y'}}{d\psi'})_{c.g.}$  with wing position. Rectangular N.A.C.A. 23012 wing alone and in combination with circular fuselage with and without fin;  $\beta_r, 0^\circ$ ;  $\alpha, 5^\circ$ .